CONFIDENTIAL

OCT 18 1956

9/18232

ITR-1345

Copy No. 199 A

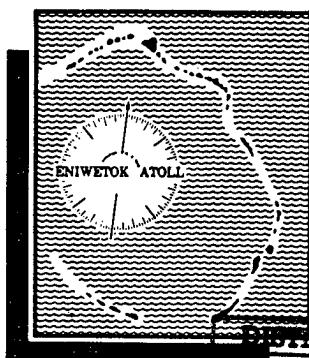(No WT issued.)

PRELIMINARY REPORT

# *Operation*
# REDWING

## PACIFIC PROVING GROUNDS

May - July 1956

Classification (Cancelled) (Changed to ~~CONFIDENTIAL~~
By Authority of DASASC-3 memo: 3/26/62
By _____ Date 4/3/62

### GAMMA RAYS FROM PLANE AND VOLUME SOURCE DISTRIBUTIONS

19960702 081

ENIWETOK ATOLL

DISTRIBUTION STATEMENT A
Approved for public release
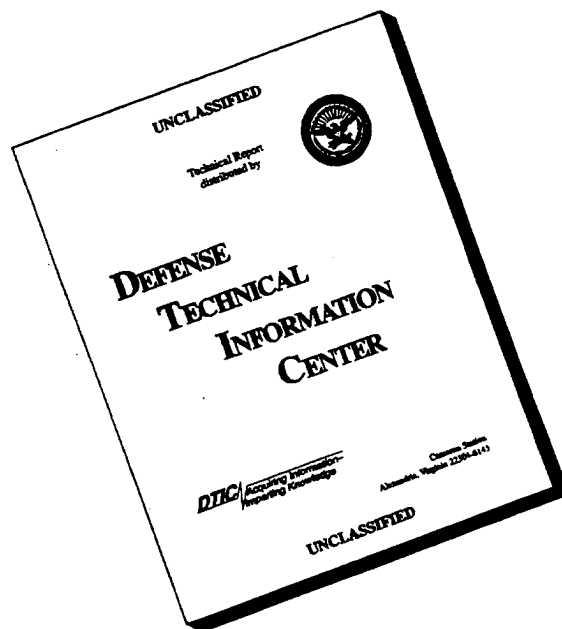Distribution Unlimited

HEADQUARTERS FIELD COMMAND, ARMED FORCES SPECIAL WEAPONS PROJECT

SANDIA BASE, ALBUQUERQUE, NEW MEXICO

DECLASSIFIED BY DNA ISTS PER NTPR
REVIEW. DISTRIBUTION STATEMENT "A"
APPLIES.

_____ DATE 10/20/95

CONFIDENTIAL

# DISCLAIMER NOTICE

UNCLASSIFIED

Technical Report
distributed by

DEFENSE
TECHNICAL
INFORMATION
CENTER

DTIC Acquiring Information—
Imparting Knowledge

Alexandria, Virginia 22304-6145

UNCLASSIFIED

THIS DOCUMENT IS BEST
QUALITY AVAILABLE. THE
COPY FURNISHED TO DTIC
CONTAINED A SIGNIFICANT
NUMBER OF PAGES WHICH DO
NOT REPRODUCE LEGIBLY.

ISST

29 January 1996

MEMORANDUM FOR DEFENSE TECHNICAL INFORMATION CENTER
ATTENTION: OCD/Mr. Bill Bush

SUBJECT: Declassification of ITR-1345

The Defense Nuclear Agency Security Office (OPSSI) **has declassified** the following report:

ITR-1345
Preliminary Report
Operation REDWING
Pacific Proving Grounds
May-July 1956
Gamma Rays From Plane and Volume Source
Distributions.

Distribution statement **"A"** applies.

Since this report does not have a final issue, this office has enclosed a copy for NTIS' system. Please inform DNA of the assigned accession number.

Enclosure:
A/S

JOSEPHINE B. WOOD
Chief, Technical Support Branch

DTIC QUALITY INSPECTED 4

This is a preliminary report based on all data available at the close of this project's participation in Operation REDWING. The contents of this report are subject to change upon completion of evaluation for the final report. This preliminary report will be superseded by the publication of the final (WT) report. Conclusions and recommendations drawn herein, if any, are therefore tentative. The work is reported at this early time to provide early test results to those concerned with the effects of nuclear weapons and to provide for an interchange of information between projects for the preparation of final reports.

When no longer required, this document may be destroyed in accordance with applicable security regulations. When destroyed, notification should be made to

AEC Technical Information Service Extension
P. O. Box 401
Oak Ridge, Tenn.

DO NOT RETURN THIS DOCUMENT

This document consists of 38 pages

No. 159 of 265 copies, Series A

OPERATION REDWING — PRELIMINARY REPORT

SEPTEMBER 1956

# GAMMA RAYS FROM PLANE AND VOLUME SOURCE DISTRIBUTIONS

Victor A. J. van Lint

Program 2 Staff
Weapons Effects Tests
Field Command
Armed Forces Special Weapons Project
Sandia Base
Albuquerque, New Mexico

Approved:

*L. L. Woodward*

L. L. Woodward, Col, USAF
Technical Director

*Kenneth D. Coleman*

K. D. Coleman, Col, USAF
Commander, Task Unit 3

*D. C. Campbell*

D. C. Campbell, CDR, USN
Director, Program 2

SUMMARY OF SHOT DATA, OPERATION REDWING

| Shot Name (Unclassified) | Date (PPG) | Time (Approximate) | Location | Type | H&N Coordinates (Actual Ground Zero) | Geographic ° ' " |
|---|---|---|---|---|---|---|
| Lacrosse | 5 May | 0629 | Eniwetok Yvonne | Surface Land | 124515 E 106885 N | 11 33 29 / 162 21 18 |
| Cherokee | 21 May | 0551 | Bikini Off Charlie | Air Drop (4320±150 ft) Over Water | 96200 ± 100 E 185100 ± 500 N | 11 43 50 / 165 19 46 |
| Zuni | 28 May | 0556 | Bikini Tare | Surface Land Water | 110309 E 100154 N | 11 29 48 / 165 22 09 |
| Yuma | 28 May | 0756 | Eniwetok Sally | 200-ft Tower | 112155 E 130604 N | 11 37 24 / 162 19 13 |
| Erie | 31 May | 0615 | Eniwetok Yvonne | 300-ft Tower | 127930 E 102060 N | 11 32 41 / 162 21 52 |
| Seminole | 6 June | 1255 | Eniwetok Irene | Surface Land[a] | 75237 E 149897 N | 11 40 35 / 162 13 02 |
| Flathead | 12 June | 0626 | Bikini Off Dog | Barge Water | 116768 E 164094 N | 11 40 22 / 165 23 13 |
| Blackfoot | 12 June | 0626 | Eniwetok Yvonne | 200-ft Tower | 126080 E 104435 N | 11 33 04 / 162 21 33 |
| Kickapoo | 14 June | 1126 | Eniwetok Sally | 300-ft Tower | 114018 E 132295 N | 11 37 41 / 162 19 32 |
| Osage | 16 June | 1314 | Eniwetok Yvonne | Air Drop (680±35 ft) Over Land | 126647 ± 50 E 102851 ± 50 N | 11 32 48 / 162 21 39 |
| Inca | 22 June | 0956 | Eniwetok Pearl | 200-ft Tower | 105300 E 135540 N | 11 37 53 / 162 18 04 |
| Dakota | 26 June | 0606 | Bikini Off Dog | Barge Water | 116767 E 164097 N | 11 40 22 / 165 23 13 |
| Mohawk | 3 July | 0606 | Eniwetok Ruby | 300-ft Tower | 109737 E 132165 N | 11 37 39 / 162 18 49 |
| Apache | 9 July | 0606 | Eniwetok Flora | Barge Water | 69227 E 148063 N | 11 40 17 / 162 12 01 |
| Navajo | 11 July | 0556 | Bikini Off Dog | Barge Water | 116816 E 160604 N | 11 39 48 / 165 23 14 |
| Tewa | 21 July | 0546 | Bikini Charlie-Dog Reef | Barge Water | 99776 E 164476 N | 11 40 26 / 165 20 22 |
| Huron | 22 July | 0616 | Eniwetok Flora | Barge Water | 70015 E 148304 N | 11 40 19 / 162 12 09 |

a See ITR-1344 for further details.

Bikini Atoll. Locations of test detonations during Operation REDWING
are indicated by large lettering and arrows. Native island names
with corresponding military identifiers are given in the tabulation.
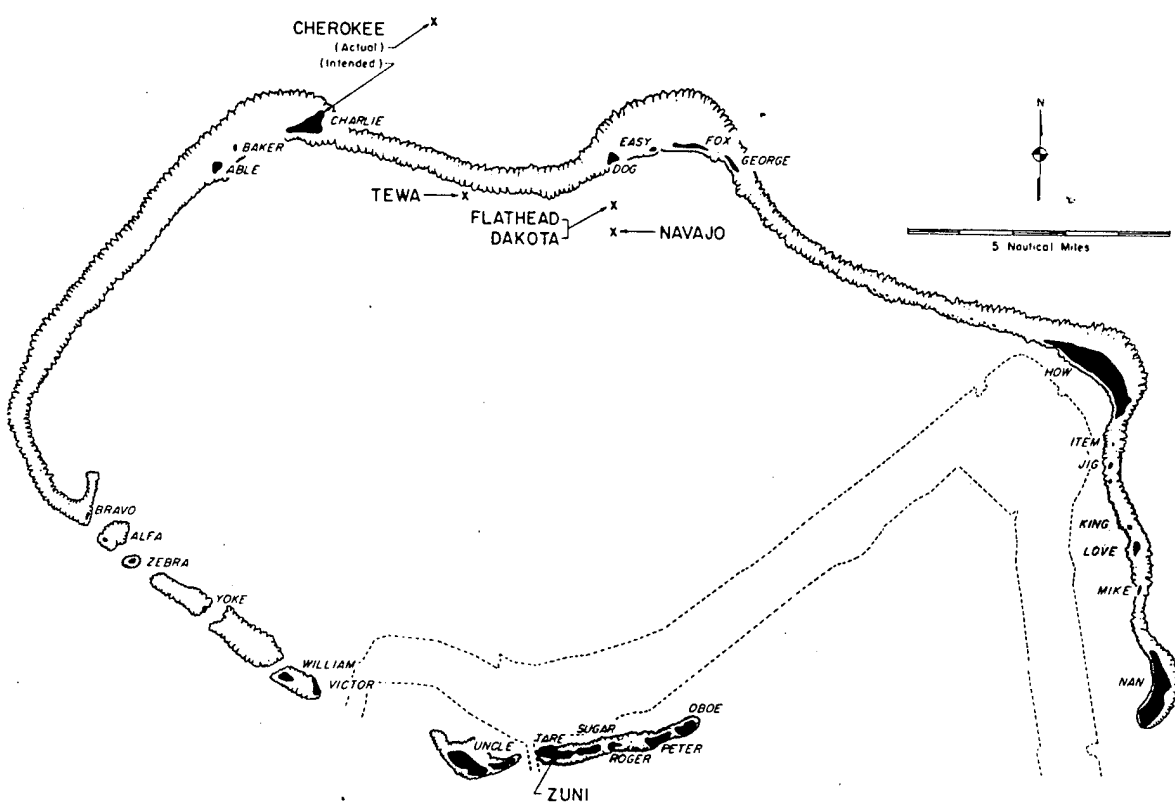
| | | | | | | | |
|---|---|---|---|---|---|---|---|
| Airukiiji | Oboe | Bokoaetokutoku | Alfa | Eniirikku | Uncle | Rochikarai | Love |
| Airukiraru | Peter | Bokobyaadaa | Able | Eninman | Tare | Romurikku | Fox |
| Aomoen | George | Bokonejien | Baker | Enyu | Nan | Rukoji | Victor |
| Arriikan | Yoke | Bokonfuaaku | Item | Ionchebi | Mike | Uorikku | Easy |
| Bigiren | Roger | Bokororyuru | Bravo | Namu | Charley | Yomyaran | Jig |
| Bikini | How | Chieerete | William | Ourukaen | Zebra | Yurochi | Dog |
| | | Eniairo | King | Reere | Sugar | | |

Huron    22 July    0616    Eniwetok Flora    Water    14°8304 N    162 12 09

Eniwetok Atoll. Locations of test detonations during Operation REDWING are indicated by large lettering and arrows. Native island names with corresponding military identifiers are given in the tabulation.

| Aaraanbiru | Vera | Chinieero | Alvin | Igurin | Glenn | Ribaion | James |
|---|---|---|---|---|---|---|---|
| Aitsu | Olive | Chinimi | Clyde | Japtan | David | Rigili | Leroy |
| Aniyaanii | Bruce | Cochita | Daisy | Kirinian | Lucy | Rojoa | Ursula |
| Aomon | Sally | Coral Heads | Mack, Oscar | "M" | Zona | Ruchi | Clara |
| Biijiri | Tilda | Eberiru | Ruby | Mul | Henry | Rujoru | Pearl |
| Bogairikk | Helen | Elugelab | Flora | Muzin | Kate | Runit | Yvonne |
| Bogallua | Alice | Engebi | Janet | Parry | Elmer | Sandildefonso | Edna |
| Bogombogo | Belle | Eniwetok | Fred | Piiraai | Wilma | Teiteiripucchi | Gene |
| Bogon | Irene | Girilnien | Keith | Pokon | Irwin | Yeiri | Nancy |
| Bokonaarappu | Mary | | | | | | |

4

# ABSTRACT

Calculations have been performed for the gamma-ray dose rate: (1) inside a uniformly contaminated volume, as in a radioactive cloud or in contaminated water; (2) as a function of altitude above the center of a uniformly contaminated circular island; and (3) as a function of altitude above uniformly contaminated water.

The calculations have been performed for monoenergetic sources of 0.15, 0.30, 0.60, 1.2, and 2.5 Mev and for some experimentally observed fallout spectra.

# FOREWORD

This report presents the results of a special study undertaken in connection with the fallout program of Operation REDWING to provide a theoretical basis for analysis of the experimental results of Projects 2.61 through 2.66. Since a field instrumentation effort was not involved, this report does not carry a project number, and will not be replaced by a WT-series final report.

For readers interested in other pertinent test information, reference is made to ITR-1344, Summary Report of the Commander, Task Unit 3. This summary report includes the following information of general interest: (1) an overall description of each detonation, including yield, height of burst, ground zero location, time of detonation, and ambient atmospheric conditions at detonation; (2) a discussion of all project results; (3) a summary of each project, including objectives and results; and (4) a complete listing of all reports covering the Military Effects Program.

CONTENTS

# CHAPTER 1

## INTRODUCTION

There are two basic techniques for a field determination of the distribution of radioactive emitters in a medium: (1) securing samples of radioactive material from various portions of the medium and analyzing these samples with standard laboratory counting equipment and (2) making a radiation survey near the actual distribution of emitters. The first technique is the more accurate, but it involves long time delays associated with careful collection of samples, transportation to a laboratory, and subsequent standard geometry counting. The survey technique has been applied extensively during tests of nuclear weapons to the problem of delineating fallout areas on land and determining contamination levels for Radiological Safety purposes. It has also been applied to determine the distribution of radioactive material in the ocean and in the radioactive cloud following a nuclear detonation.

The purpose of the calculations which follow is to establish the relation between the gamma dose rate measured by a survey reading at a specified location and the density of radioactive emitters in the assumed distribution. In this presentation the dose rate will be defined as the radiation field measured in r/hr — namely, the ionization rate per unit volume of STP air. The actual situations under which such measurements are performed can be approximated by three ideal cases in which the dose rate is taken: (1) within an infinite medium uniformly populated with radioactive sources; (2) above the center of a circular disk containing a uniform surface distribution of sources; or (3) in a semi-infinite medium at various distances from the interface with the complementary semi-infinite medium, having a different composition, which has radioactive sources uniformly distributed throughout its volume.

The first case corresponds to the measurement of the dose rate within a nuclear cloud or within water in which radioactive fallout has been mixed. The second applies approximately to the problem of determining the contamination of the surface of an island by a measurement of the dose rate above its center. The large land-source problem is that in which the radius of the disk is allowed to become infinite. The third case corresponds to the measurement of the dose rate in the air above contaminated ocean water.

The actual calculations are performed for the following monoenergetic sources: 150 kev, 300 kev, 600 kev, 1.2 Mev, and 2.5 Mev. The data which may then be used to compute the absorption relations for any spectrum, are applied to some experimentally observed fallout spectra.

# CHAPTER 2

## BASIC THEORY

### 2.1 INTERACTIONS OF GAMMA RAYS

Gamma rays of moderate energy interact with matter by the following three mechanisms:

1. Photoelectric Absorption. The gamma ray ejects an electron from an atom, imparting its total energy to the electron. The gamma ray disappears, and the energy is locally distributed by ionizing and exciting collisions of the electron.

2. Compton Scattering. The gamma ray imparts a portion of its energy to an electron and a scattered gamma ray of lower energy travels in a new direction. The energy of the electron is locally distributed, but the scattered gamma ray contributes to the resultant gamma dosage elsewhere.

3. Pair Production. A high-energy (>1.02 Mev) gamma ray can interact with an electric field to produce an electron-positron pair. The gamma ray disappears, and the kinetic energy of the electron and positron are locally distributed. The subsequent annihilation of the positron produces two gamma rays of 0.511-Mev energy which travel in opposite but arbitrary directions and contribute to the total gamma dosage elsewhere.

Each of the above interactions has a certain probability ($\mu_1$, $\mu_2$, $\mu_3$) of occurring per unit path length of a gamma ray in a given medium. The probability that any of the interactions occurs per unit path length is then $\mu_0 = \mu_1 + \mu_2 + \mu_3$ and the probability that the gamma ray has not interacted in a distance $X = e^{-\mu_0 X}$.

### 2.2 CALCULATION OF DOSE RATE

The dose rate at a particular point in a radiation field is defined as the number of ion pairs produced per unit volume of air (STP) located at that point. The number of ion pairs produced is proportional to the energy lost per unit volume. Therefore, if the flux[1] of particles of

---

[1] Defined as the number of gammas per unit time crossing a unit area perpendicular to their direction of motion.

energy $E_o$ at the point is $F_o$ and the average fraction of the energy lost per unit distance[1] is $h_o$, then the dose rate (in r/hr) is:

$$D_o = C \, E_o \, h_o \, F_o \qquad\qquad (2.1)$$

Where: $C = 0.058$; factor to convert from energy (Mev) deposited per unit volume ($cm^3$) per second to roentgens per hour.

## 2.3  DOSE BUILDUP

The dose rate at a distance R due to the unscattered flux from a monoenergetic point source of radiation emitting $A_o$ photons per unit time can be calculated to be:

$$D_{ou} = C \, E_o \, h_o \frac{A_o}{4\pi R^2} e^{-\mu_o R} \qquad\qquad (2.2)$$

However, the dose rate is augmented by the contribution of the scattered photons. The magnitude of this dose-rate buildup has been computed for some special cases (Reference 1). The buildup factor in air has been graphed as a function of energy for various source energies (Reference 2). For the purposes of the numerical calculations involved in this report, principally to avoid tedious numerical integrations, these curves have been approximated by cubic equations:

$$B_o = 1 + b_o \, (\mu_o R) + c_o \, (\mu_o R)^2 + d_o \, (\mu_o R)^3 \qquad\qquad (2.3)$$

The coefficients have been graphed as a function of source energy $E_o$ (Figure 2.1).

It will be assumed that these same coefficients apply in the case of water, since the density effect is incorporated into $\mu_o$ and the mean atomic number is not greatly different from that of air.

The foregoing buildup factors were calculated ones and include contributions from the entire gamma spectrum below $E_o$. However, actual survey instruments usually do not detect radiation below a certain energy, usually 60 to 75 kev. Therefore, the fraction of the scattered dose contributed by such low-energy gammas was estimated using the curves in Reference 1, and this amount was subtracted from the calculated dose rate. Effectively, this procedure amounted to multiplying $b_o$, $c_o$, and $d_o$ by a factor less than one representing the fraction of the scattered dose contributed by detectable gammas.

During the solution of Case 3, it is necessary to evaluate the actual scattered flux penetrating the interface, rather than the dose rate. The curves presented in Reference 1 were again used to convert the scattered dose rate to flux as a function of energy. The method

---

[1] $h_o = \mu_1 + f_2 \mu_2 + f_3 \mu_3$ where $f_2$ and $f_3$ are the average fractions of the initial energy deposited locally for Compton scattering and pair production, respectively.
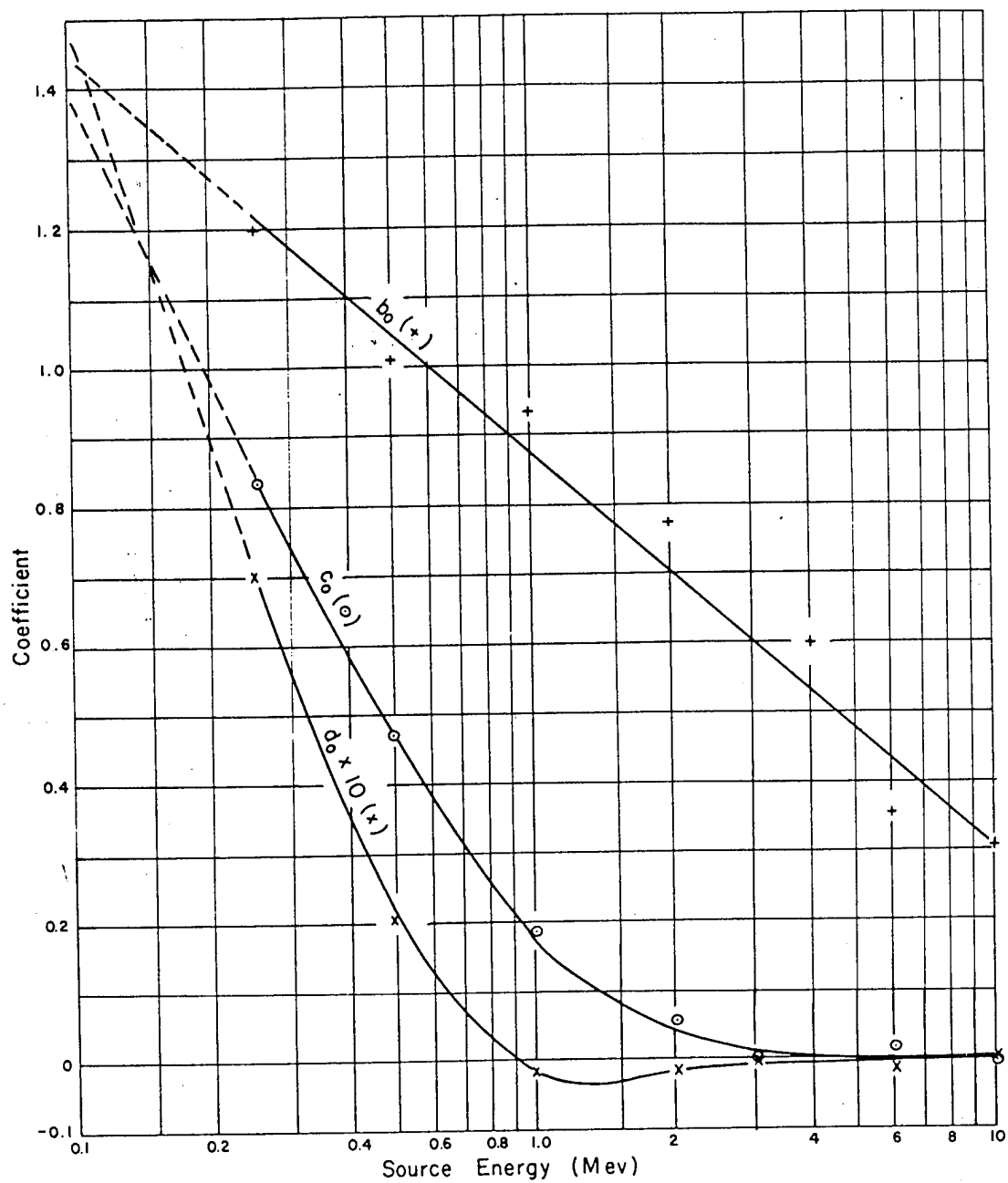
Figure 2.1  Buildup factor coefficients.

$$B_o = 1 + b_o(\mu_o R) + c_o(\mu_o R)^2 + d_o(\mu_o R)^3$$

12

used was to approximate the scattered spectrum by a sum of monoenergetic sources of energies 0.15, 0.30, 0.60, 1.2, and 2.5 Mev, where the relative strengths of these sources were determined by evaluating areas under the energy-flux curves of Reference 1. For this purpose the variation of h with energy was neglected, since it does, in fact, deviate from an average value, $\bar{h}$, by less than 15 percent.

# CHAPTER 3

## FORMULAS

### 3.1 DOSE RATE IN AN INFINITE MEDIUM

The dose rate at P due to a monoenergetic volume density of activity, $A_{vo}$, at $(R, \theta, \phi)$ is:

$$dD_O = \underbrace{B_o(\mu_o R)}_{\substack{\text{dose} \\ \text{buildup}}} \ \underbrace{C \ E_o \ h_o}_{\substack{\text{dose} \\ \text{factors}}} \ A_{vo} \ \underbrace{R^2 \sin\theta \ d\theta d\phi \ dR}_{\text{volume}} \ \underbrace{e^{-\mu_o R}}_{\text{absorption}} \ \underbrace{\frac{1}{4\pi R^2}}_{\substack{\text{solid} \\ \text{angle}}} \qquad (3.1)$$
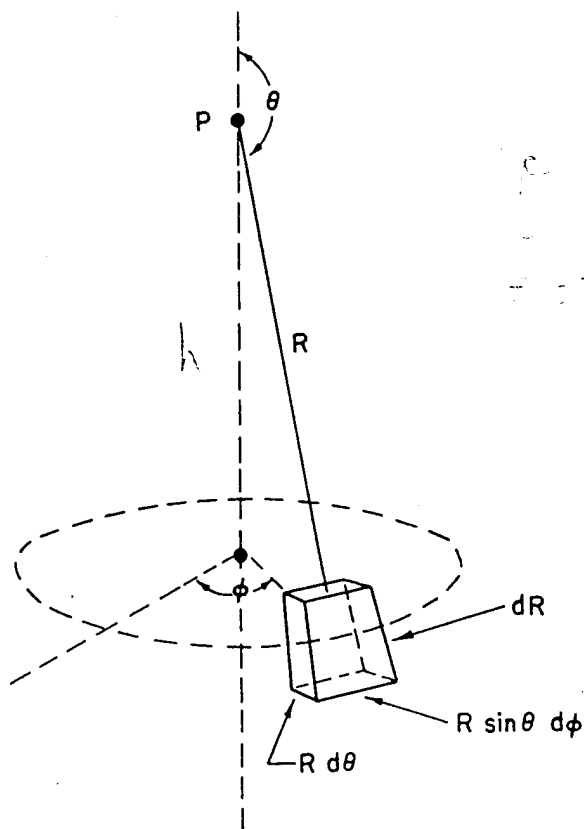
Inserting the assumed cubic equation for the buildup factor and integrating over all space variables, the total dose rate is derived to be:
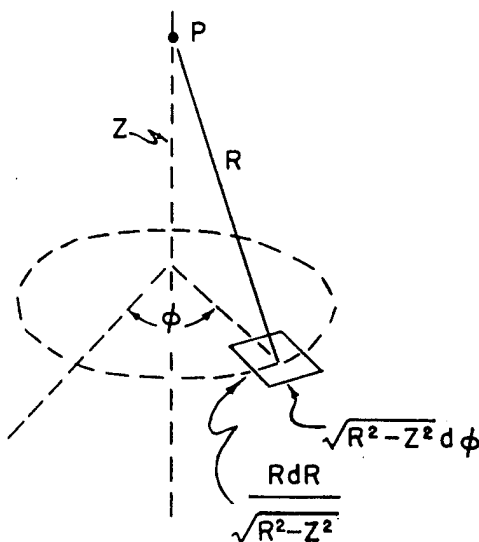
$$D_0 = C \, E_0 \, h_0 \, \frac{A_{vo}}{\mu_0} \quad (1 + b_0 + 2c_0 + 6d_0) \tag{3.2}$$

When the sources emit a spectrum of gamma rays, the above dose rate must be integrated over the energy spectrum.

## 3.2 DOSE RATE ABOVE CENTER OF CIRCULAR DISK

The dose rate at point P due to a monoenergetic uniform surface density, $A_{so}$, of isotropic sources at $(R, \phi)$ is:

$$dD_0 = B_0(\mu_0 R) \; C \, E_0 \, h_0 \, A_{so} \; R \, dR \, d\phi \; e^{-\mu_0 R} \; \frac{1}{4\pi R^2} \tag{3.3}$$



If the sources of the radiation do not emit isotropically, the quantity $\dfrac{A_{so}}{4\pi}$ should be replaced by the number of photons emitted per unit time, per unit surface area, per unit solid angle in the particular direction.

15

For isotropic emitters, the dose rate integrated over $\phi$ and up to the edge of a disk of radius $\rho$ is:

$$D_o(Z,\rho) = C \, E_o \, h_o \, \frac{A_{so}}{2} \left[ K(\mu_o Z) - K\left( \mu_o \sqrt{Z^2 + \rho^2} \right) \right] \qquad (3.4)$$

Where: $\quad K(X) = -\mathcal{E}_i(-X) + e^{-X} \left[ (b_o + c_o + 2d_o) + X \, (c_o + 2d_o) + X^2 \, d_o \right]$

$$-\mathcal{E}_i(-X) = \int_X^{\infty} \frac{e^{-t}}{t} \, dt, \text{ is the usual exponential integral.}$$

For heights large compared to the radius of the source field $(Z >> \rho)$, this formula approaches the formula for a point source having the full strength of the disk at a distance Z, namely:

$$D_o(Z,\rho)_{\overrightarrow{Z >> \rho}} \qquad C \, E_o \, h_o \quad \frac{A_{so} \, \rho^2}{4 \, Z^2} \, e^{-\mu_o Z} \left[ 1 + b_o(\mu_o Z) + \right.$$

$$\left. c_o(\mu_o Z)^2 + d_o(\mu_o Z)^3 \right] \qquad (3.5)$$

One interesting and useful result demonstrated by the above derivation is related to the fact that the two K factors are functions of the slant range to the near and far points of the contaminated circle and do not depend on any other distance. In particular, a calculation of the dose rate on the surface at the center of an uncontaminated circle of radius $\rho$ amidst an infinite contaminated plane yields the same answer as the dose rate at a height $\rho$ above an infinite contaminated plane, since both are proportional to $K(\mu_o \rho)$.

The foregoing solution actually corresponds to a contaminated plane in an infinite isotropic medium and thus differs slightly from the ground-air problem in which the medium does differ on the two sides of the plane. This fact affects the dose rate in the air through two mechanisms: (1) the effective atomic number of the ground is somewhat different from that of the air; therefore, the absorption and scattering cross sections are different and (2) the scale of the scattered trajectories is foreshortened by the greater density of the soil and thus affects the dose rate for finite-size source fields. Actually the error caused by the isotropic-medium assumption is probably less than 15 percent.

The fact that the above formula becomes logarithmically infinite as the detector approaches the surface is associated with the mathematical assumption that the vertical dimension of the detector is small compared

16

to its distance from the plane; hence, a finite number of sources are at distance zero from the detector.

## 3.3 DOSE RATE IN AIR ABOVE CONTAMINATED WATER

The solution of the air-above-water problem is performed in two steps: (1) the method of Section 3.1 is utilized to calculate the flux crossing the water surface and (2) this flux is inserted into the differential formula of Section 3.2 to calculate the effect of the air absorption.

In both steps of this solution the same assumption as that discussed in Section 3.2 must be made, i.e., the dose-buildup characteristics in a semi-infinite medium bounded by another different semi-infinite medium are the same as in a homogeneous infinite medium. In this case the errors should be small, because the effective atomic number of air and water differ but slightly and there is almost always an essentially infinite boundary surface between.

Since the effective atomic numbers do not differ greatly, the further assumption will be made that the same dose-buildup coefficients can be applied to both media. Actually, the quantity desired from the water calculation is the flux as a function of energy - not the total dose rate. Therefore, the scattered dose rate must be allocated according to the energy spectrum of the scattered radiation. In the more-general problem, where the sources emit a spectrum of gamma rays, this calculation can be represented as a modification to the primary energy spectrum.

TABLE 3.1  SCATTERED ENERGY FLUX FRACTIONS, $s_i$

| $E_o$ (Mev) \ $E_{scat}$ (Mev) | 0.15 | 0.3 | 0.6 | 1.2 | 2.5 | $<0.75$ |
|---|---|---|---|---|---|---|
| 0.15 | 0.15 | | | | | 0.85 |
| 0.3 | 0.55 | 0.20 | | | | 0.25 |
| 0.6 | 0.25 | 0.30 | 0.25 | | | 0.20 |
| 1.2 | 0.20 | 0.20 | 0.25 | 0.25 | | 0.10 |
| 2.5 | 0.10 | 0.10 | 0.15 | 0.35 | 0.25 | 0.05 |

The curves in Reference 1 have been used to allocate this dose rate among the various contributing energies. The energy-flux curves have been separated into intervals centered at a series of energies $E_o$, $E_o/2$, $E_o/4$, $E_o/8$, etc., with the lowest interval bounded by 75 kev. For the purpose of these calculations, the average fractional energy loss, $h$, is assumed to have a constant value of $\bar{h} = 0.33 \times 10^{-4} cm^{-1}$ over the entire range; therefore, the area under the energy-flux curves within each of the intervals measures their relative contributions to the scattered dose rate. The fraction of the total scattered flux contributed by each energy, $s_i$, computed in this manner is given in Table 3.1. Again, the part below 75 kev will be ignored, since instruments will not be sensitive to it.

In the ensuing calculations, the scattered flux has been reintroduced as an effective uniformly distributed additional source such that only the unscattered flux from the composite source need be calculated. In other words, the flux at the surface will be correctly evaluated by calculation of the unscattered radiation from the composite source distribution. From formulas derived before, the additional source strength at $E_i$ due to a source of strength $A_{vo}$ at $E_o$ is:

$$\triangle A_{vi} = s_i \frac{E_o}{E_i} \frac{\mu_i}{\mu_o} \frac{h_o}{\bar{h}} \, A_{vo}' \, (b_o + 2c_o + d_o) \qquad (3.6)$$

The effective source strength $A_{vj}^*$ at energy $E_j$ can then be calculated by adding the real source, $A_j$, to all terms $\triangle A_{vj}$ due to primary source of energy $E_o \geq E_j$.

The angular distribution of the scattered radiation will be assumed to be the same as that of the unscattered radiation, since this corresponds to isotropy in the upper hemisphere.

Using the method of Section 3.1, the number of unscattered photons due to a source $A_{vo}^*$ per unit time crossing a unit surface area at an angle $\theta$ is:

$$A_o(\theta) \, d\Omega = \int_{R=0}^{\infty} \frac{A_{vo}^*}{4\pi} e^{-\mu_{ow} R} \cos\theta \, dR \, d\Omega$$

$$= \frac{A_{vo}^*}{4\pi \mu_{ow}} \cos\theta \, d\Omega \qquad (3.7)$$

Where: $\mu_{ow}$ = Interaction coefficient of water for gammas of energy $E_o$.

The factor $\cos\theta$ arises from the fact that a unit area of the surface projects onto an area $\cos\theta$ perpendicular to the direction of flight of the photons.

As indicated in Section 3.2, quantity $A_o(\theta)$ is to be inserted instead of $\frac{A_{so}}{4\pi}$ in the differential form of the infinite plane formula.[1]

---

[1] This expression must be inserted into the differential formula because the angular dependence of the radiation coming through the surface differs from the contaminated plane case by a factor $\cos\theta$.

$$D_o(Z) = \int_{R=Z}^{\infty} \int_{\phi=0}^{2\pi} B_o(\mu_o R)\; C\, E_o\, h_o\, \frac{A_{vo}^{*}}{\mu_{ow}}\; \frac{Z_o}{R}\; \frac{e^{-\mu_o R}}{4\pi R^2}\; R\, d\phi\, dR$$

$$= C\, E_o\, h_o\, \frac{A_{vo}^{*}}{2\mu_{ow}}\; K_w\, (\mu_o Z) \qquad\qquad (3.8)$$

Where: $\quad K_w(X) = X\, \mathcal{E}_1(-X)\;\; (1-b_o) + e^{-X}\left[1 + X\,(c_o + d_o) + X^2\, d_o\right]$

This dose-rate expression must subsequently be summed over the effective source-energy spectrum, $A_{vi}^{*}$, to obtain the total dose rate. The above expression does not approach infinity as the detector approaches the interface, since the volume distribution of sources places only an infinitesimal number of them at distance zero from the detector.

If a detector having a sensitive solid angle less than $2\pi$ is used, a finite circle becomes the effective source, and the above integral should be taken to the finite upper limit $L = \dfrac{Z}{\cos\alpha}$, where $\alpha$ is the acceptance angle of the detector. The finite field $K_{wf}$ factor is then given by the following expression:

$$K_{wf}\,(\mu_o Z, \alpha) = K_w\,(\mu_o Z) - \cos\alpha\; K_w\left(\frac{\mu_o Z}{\cos\alpha}\right) \qquad\qquad (3.9)$$

# CHAPTER 4

## RESULTS OF CALCULATIONS

Calculations have been performed for monoenergetic sources of 0.15, 0.30, 0.60, 1.2, and 2.5 Mev. In addition, they have been performed for three particular gamma-ray-source spectra applicable to radioactive fallout fields resulting from nuclear detonations. The composition of these spectra in terms of the calculated energies is summarized in Table 4.1. They are applicable to: (1) fission-product activity from a fission weapon, (2) early (one-day) activity from a thermonuclear weapon, and (3) later (2-to-7-day) activity from a thermonuclear weapon.

### TABLE 4.1  ASSUMED SPECTRA

| $E_0$ (Mev) | Relative Photon Flux Percent | | |
|---|---|---|---|
| | Spectrum I | Spectrum II | Spectrum III |
| 0.15 | 15 | 25 | 50 |
| 0.3 | 20 | 25 | 25 |
| 0.6 | 45 | 24 | 20 |
| 1.2 | 15 | 24 | 4 |
| 2.5 | 5 | 2 | 1 |
| Average Energy | 0.66 Mev | 0.59 Mev | 0.34 Mev |

Table 4.2 summarizes the absolute conversion factors derived from these calculations. The surface or volume density of activity is chosen to be one curie per square meter or cubic meter, respectively.

Figures 4.1 through 4.8 present the factor to convert a reading at a height Z above a finite contaminated plane to a reading at a height of 3 feet. Figures 4.9 and 4.10 present the conversion of the 3-foot reading from a finite-plane source to an infinite-plane source having the same surface density of activity.

Figures 4.11 and 4.12 present the altitude conversion factors for the air-over-water case.

## TABLE 4.2  ABSOLUTE CONVERSION FACTORS

| $E_0$ | Infinite[a] Volume Distribution in Water of 1 curie/meter³ | | Infinite[a] Volume Distribution in Air of 1 curie/meter³ | Infinite Surface Distribution of 1 curie/meter² |
|---|---|---|---|---|
| | Dose Rate in Water | Dose Rate at 3 ft Above Water | Dose Rate in Air | Dose Rate at 3 ft Above Surface |
| Mev | r/hr | r/hr | r/hr | r/hr |
| 0.15 | 0.104 | 0.05 | 96 | 1.95 |
| 0.3 | 0.60 | 0.29 | 554 | 6.05 |
| 0.6 | 1.25 | 0.61 | 1160 | 12.1 |
| 1.2 | 2.58 | 1.28 | 2360 | 22.0 |
| 2.5 | 5.37 | 2.67 | 5040 | 39.8 |
| I | 1.36 | 0.67 | 1250 | 12.2 |
| II | 1.19 | 0.59 | 1110 | 10.6 |
| III | 0.60 | 0.29 | 560 | 6.2 |

[a]Distances large compared to $1/\mu_0$.
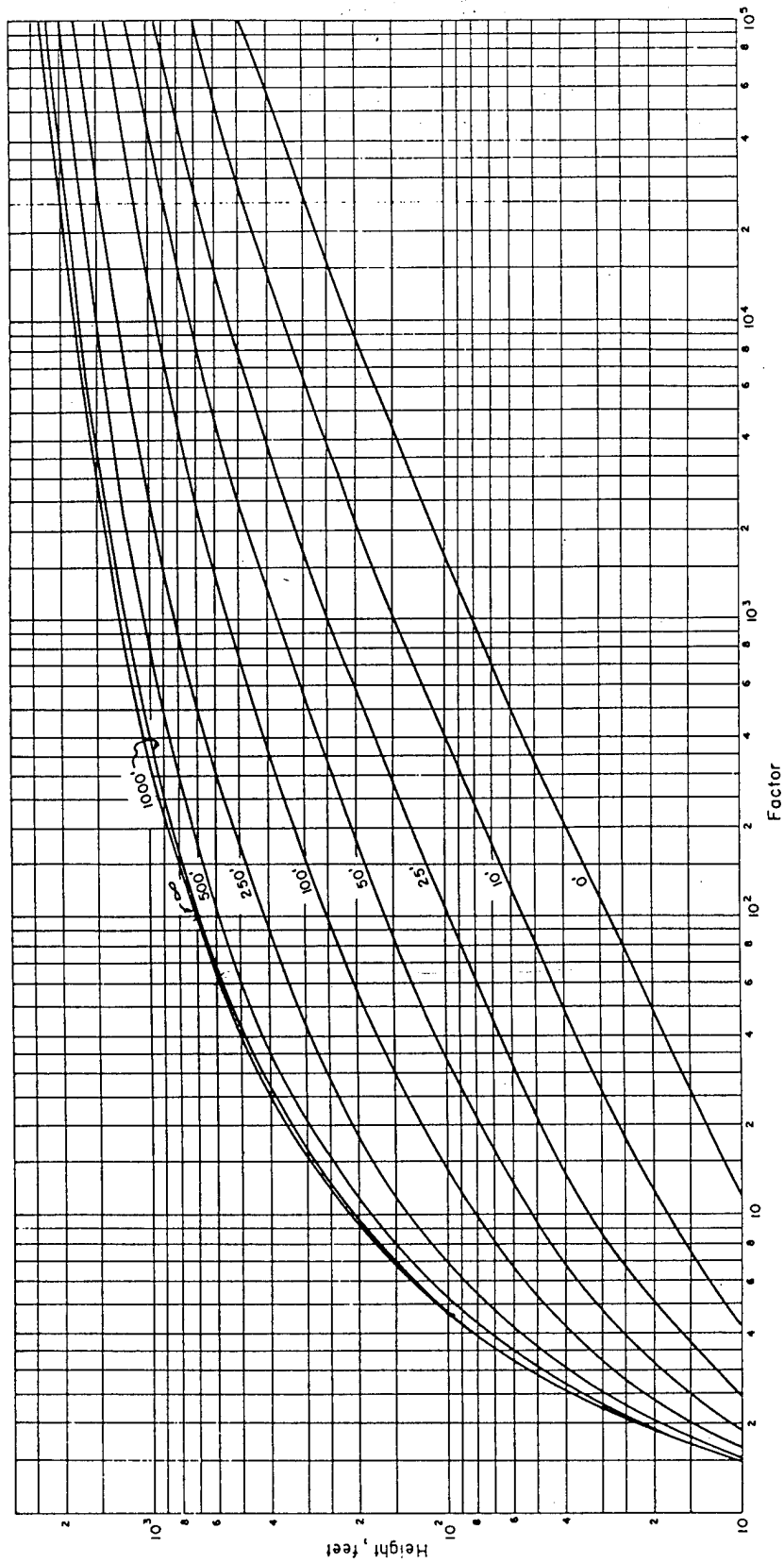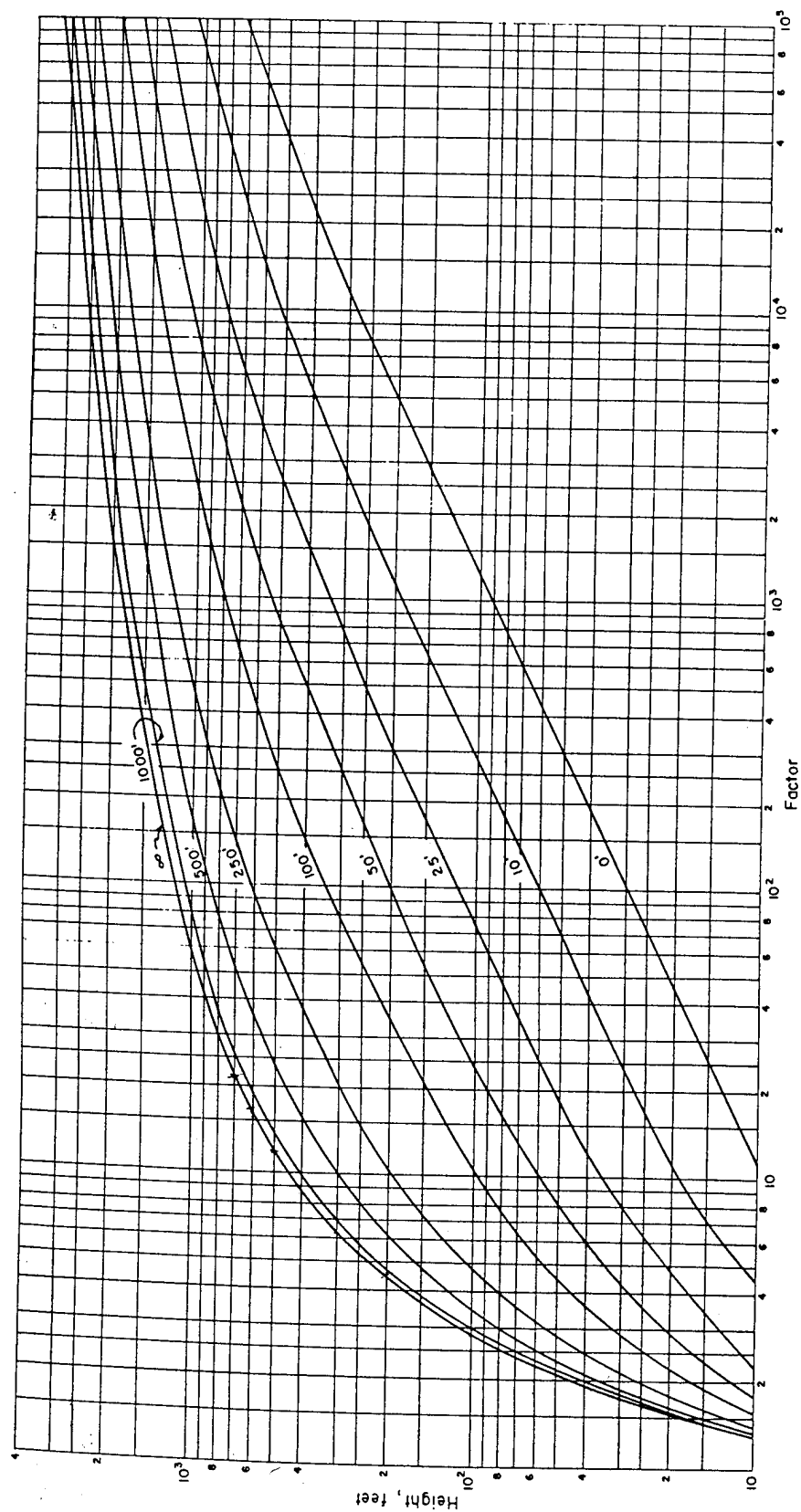
*(handwritten annotations present in margins)*

Figure 4.1 Height conversion factors over land. $E_0 = 0.15$ Mev.
(Numbers on curves refer to radius of source circle in feet)

Figure 4.2  Height conversion factors over land.  E_o = 0.3 Mev.
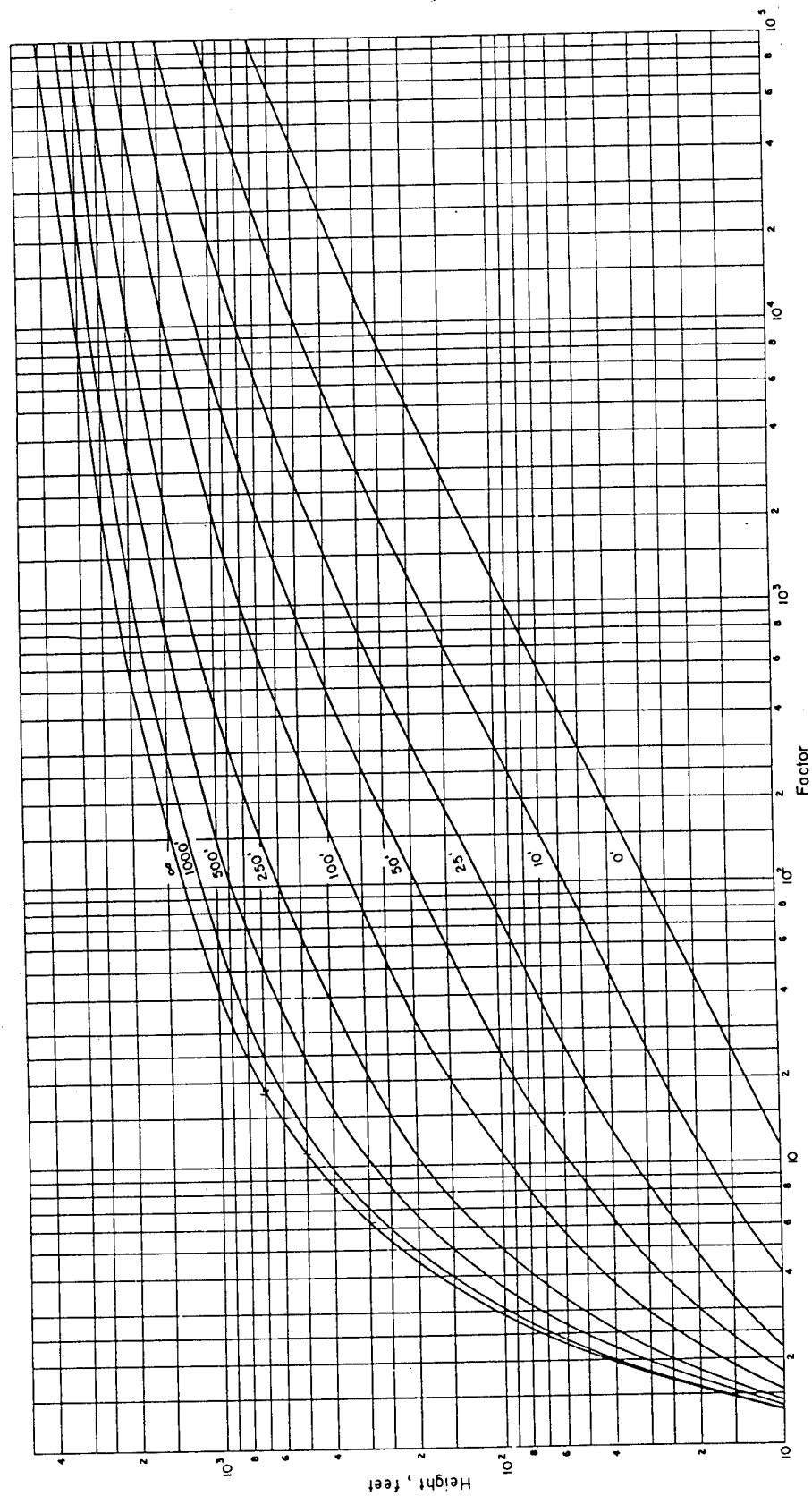(Numbers on curves refer to radius of source circle in feet)

23

Figure 4.3  Height conversion factors over land.  $E_0 = 0.6$ Mev.
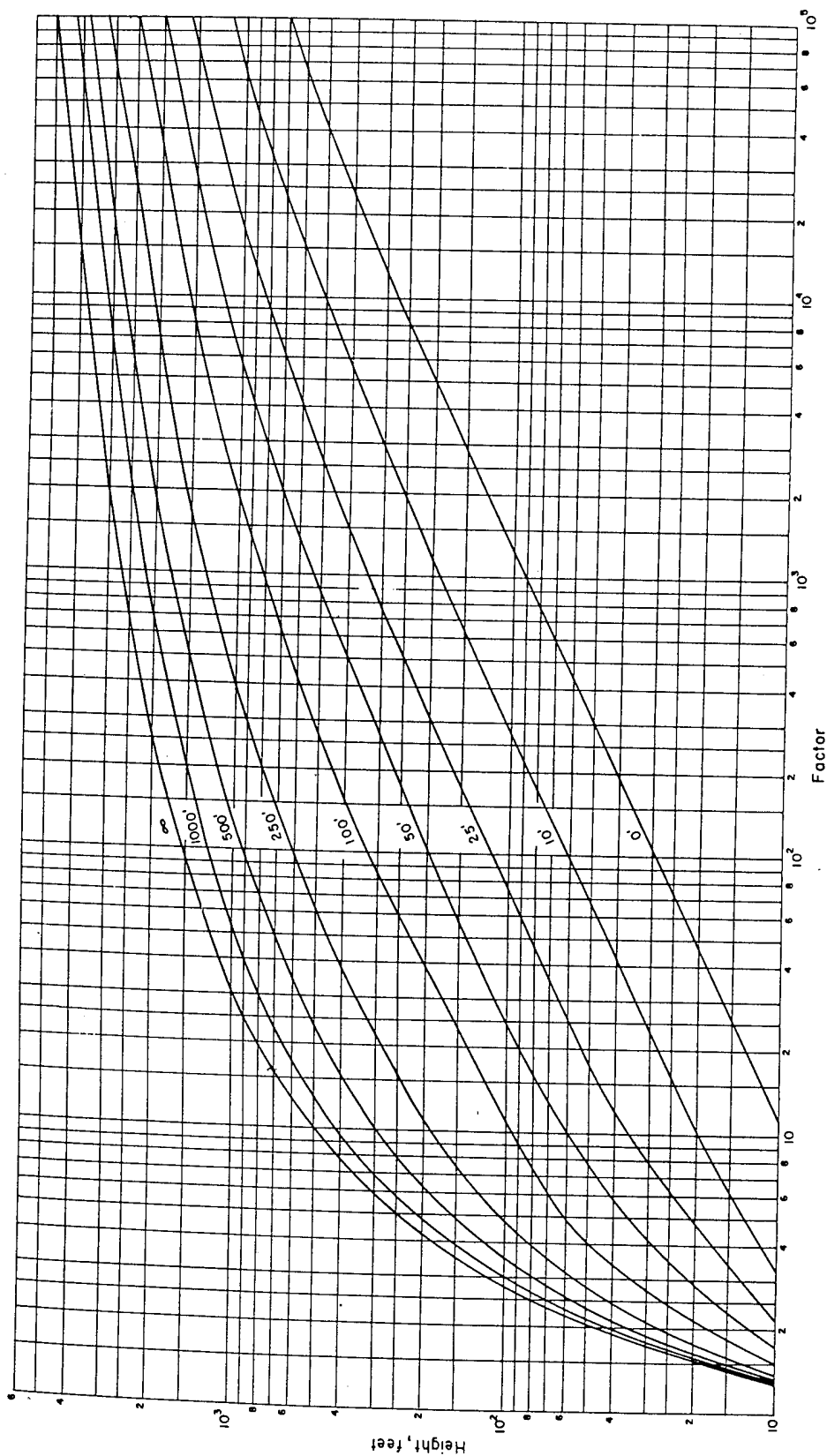(Numbers on curves refer to radius of source circle in feet)

24

Figure 4.4  Height conversion factors over land.  $E_0 = 1.2$ Mev.
(Numbers on curves refer to radius of source circle in feet)
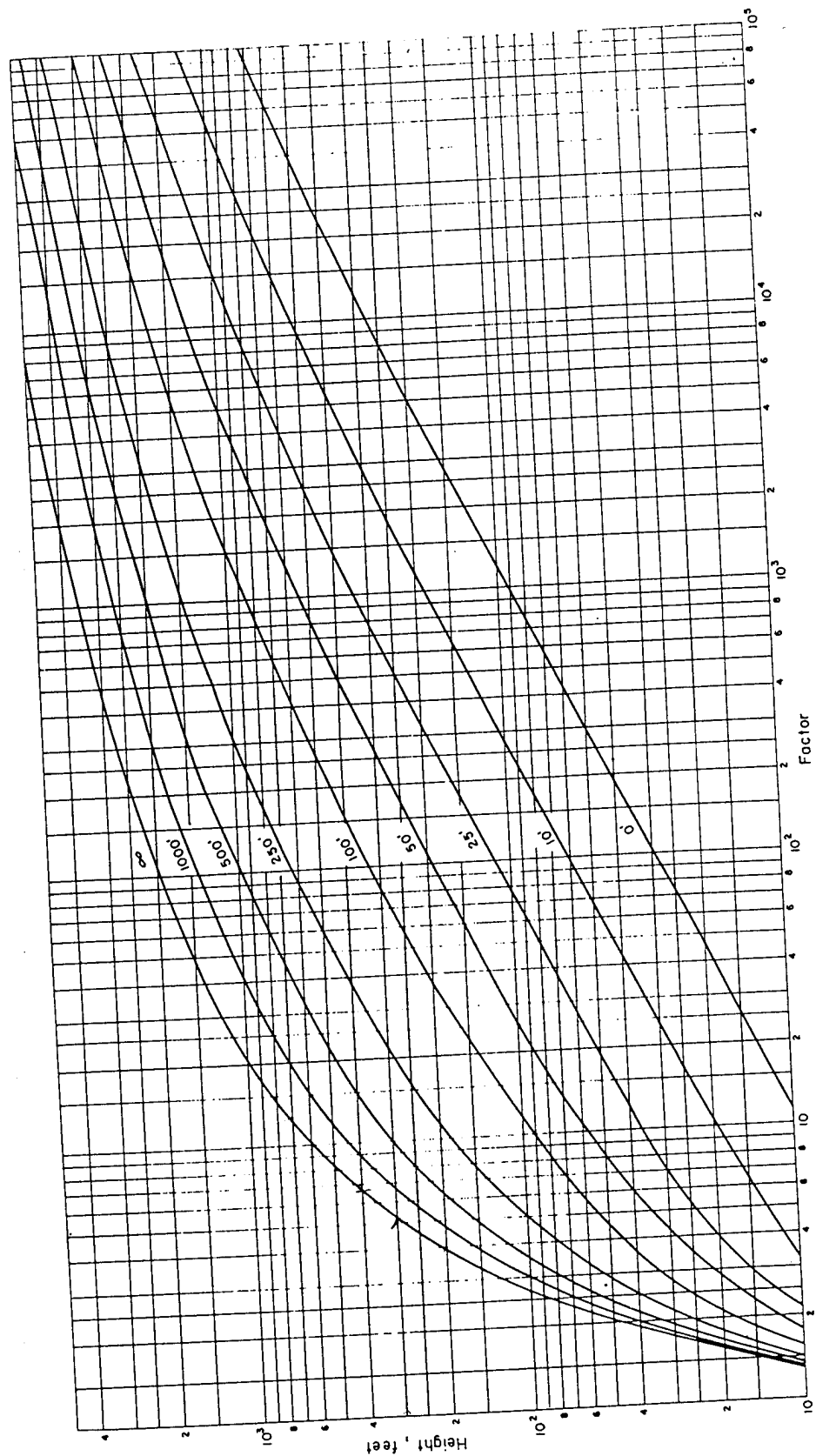
25

Figure 4.5  Height conversion factors over land.  $E_0 = 2.5$ Mev.
(Numbers on curves refer to radius of source circle in feet)
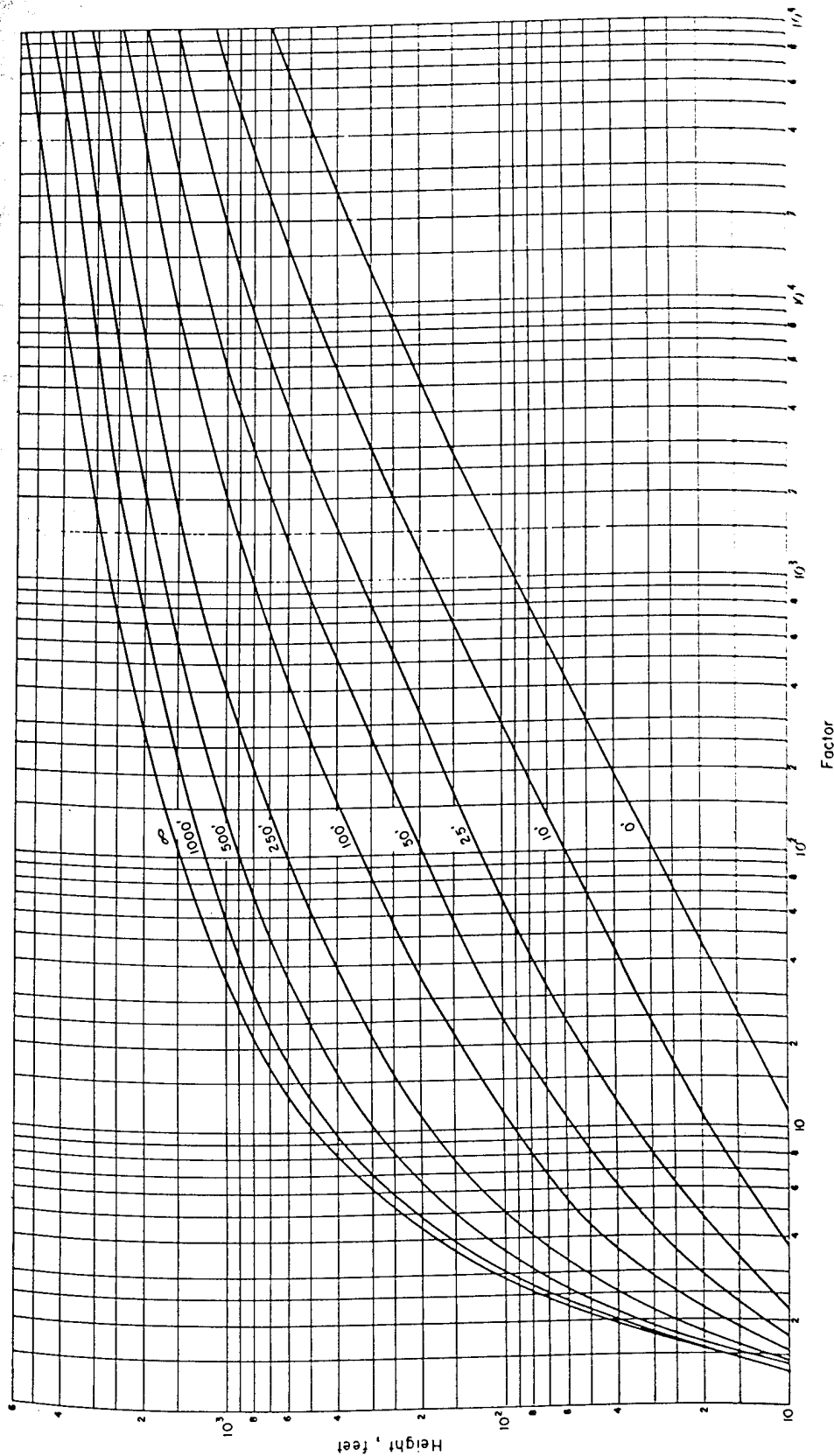
26

Figure 4.6  Height conversion factors over land.  Spectrum I.
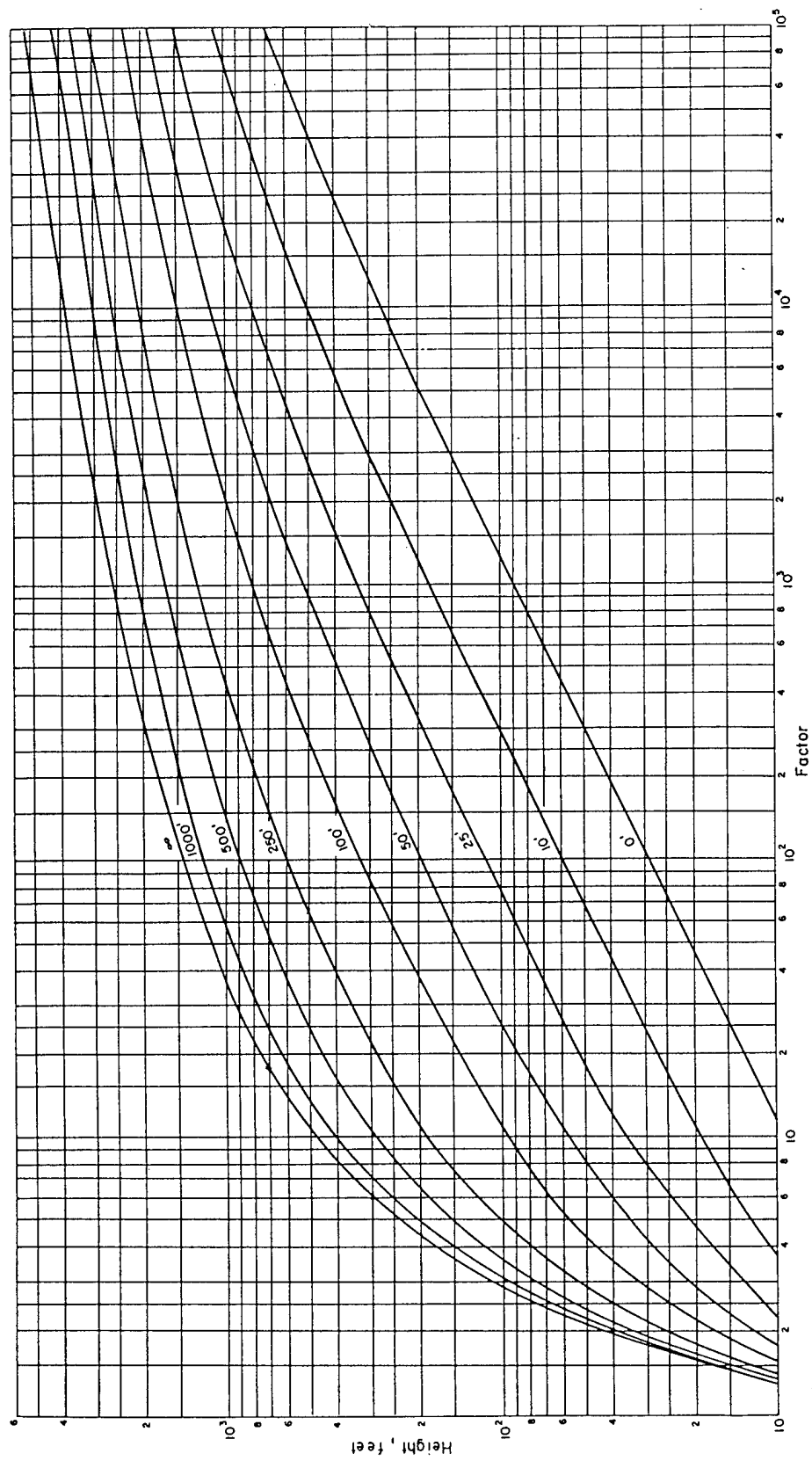(Numbers on curves refer to radius of source circle in feet)

27

Figure 4.7  Height conversion factors over land.  Spectrum II.
(Numbers on curves refer to radius of source circle in feet)
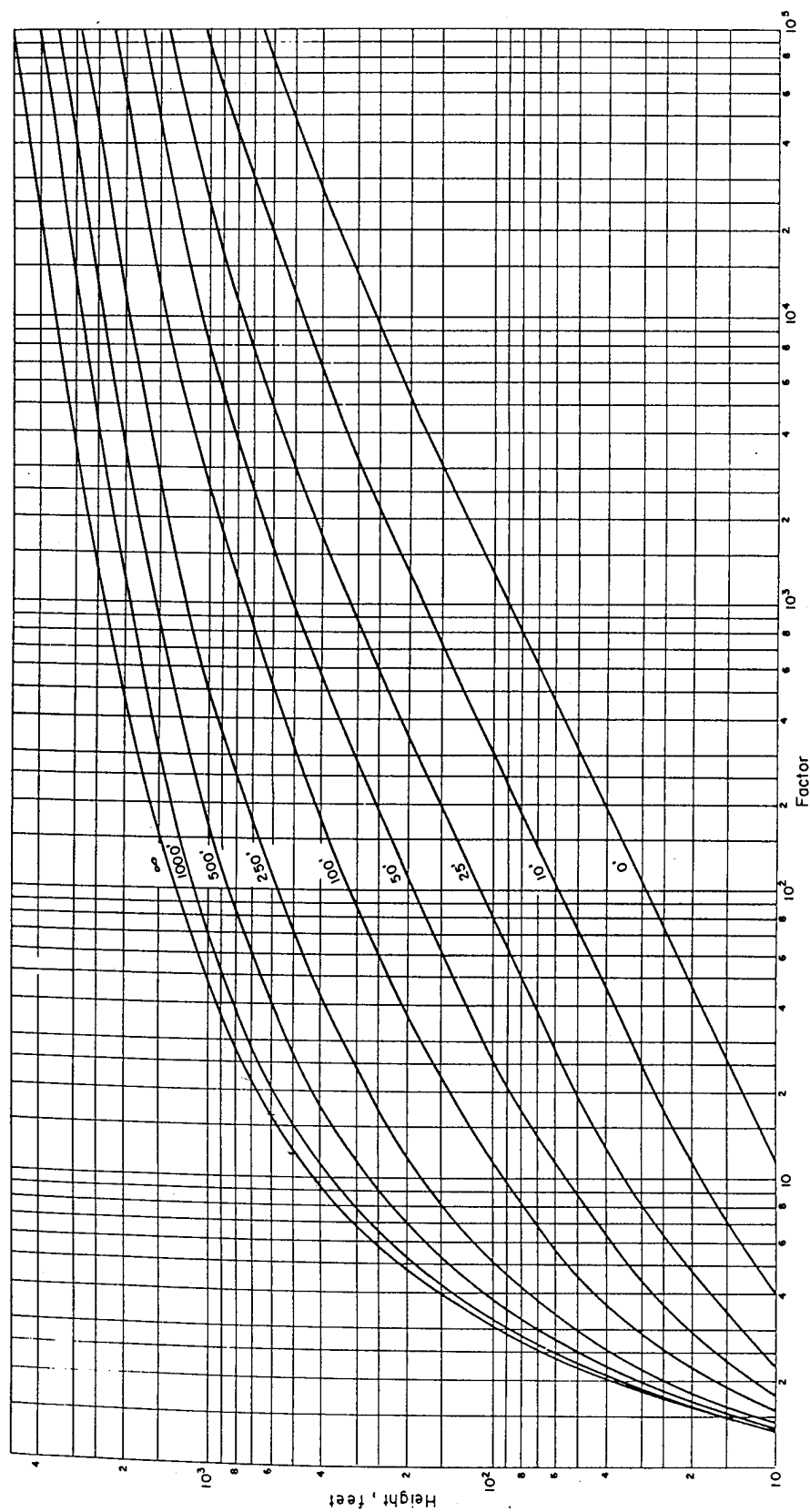
Figure 4.8 Height conversion factors over land. Spectrum III.
(Numbers on curves refer to radius of source circle in feet)

Figure 4.9  Conversion factors from finite plane
to infinite plane – monoenergetic sources.

30

Figure 4.10  Conversion factors from finite to
infinite plane.  Spectrum I, II, and III.

Figure 4.11 Height conversion factors over water — monoenergetic sources.

32

Figure 4.12  Height conversion factors over water.  Spectrum I, II, and III.

# CHAPTER 5

## DISCUSSION

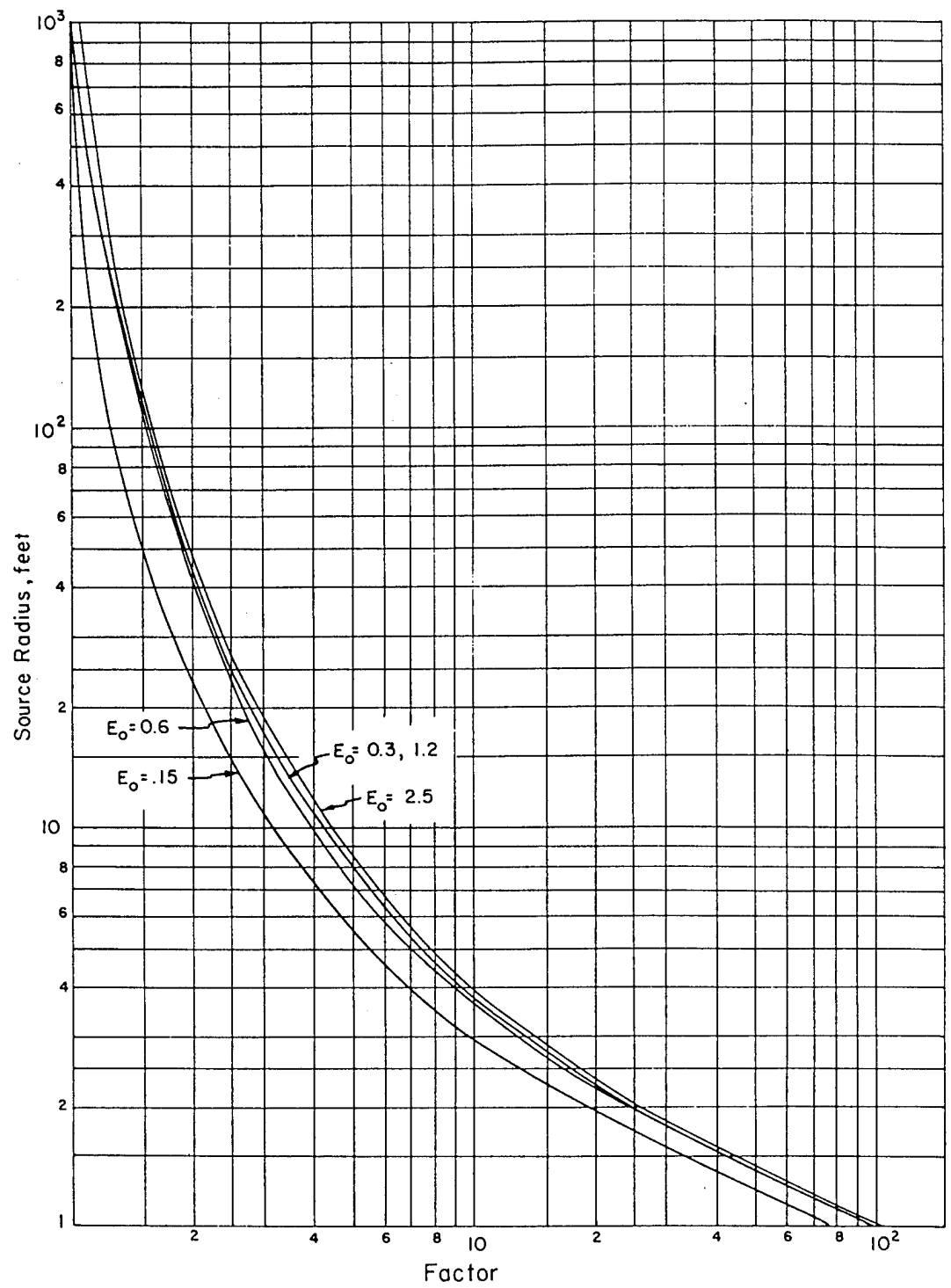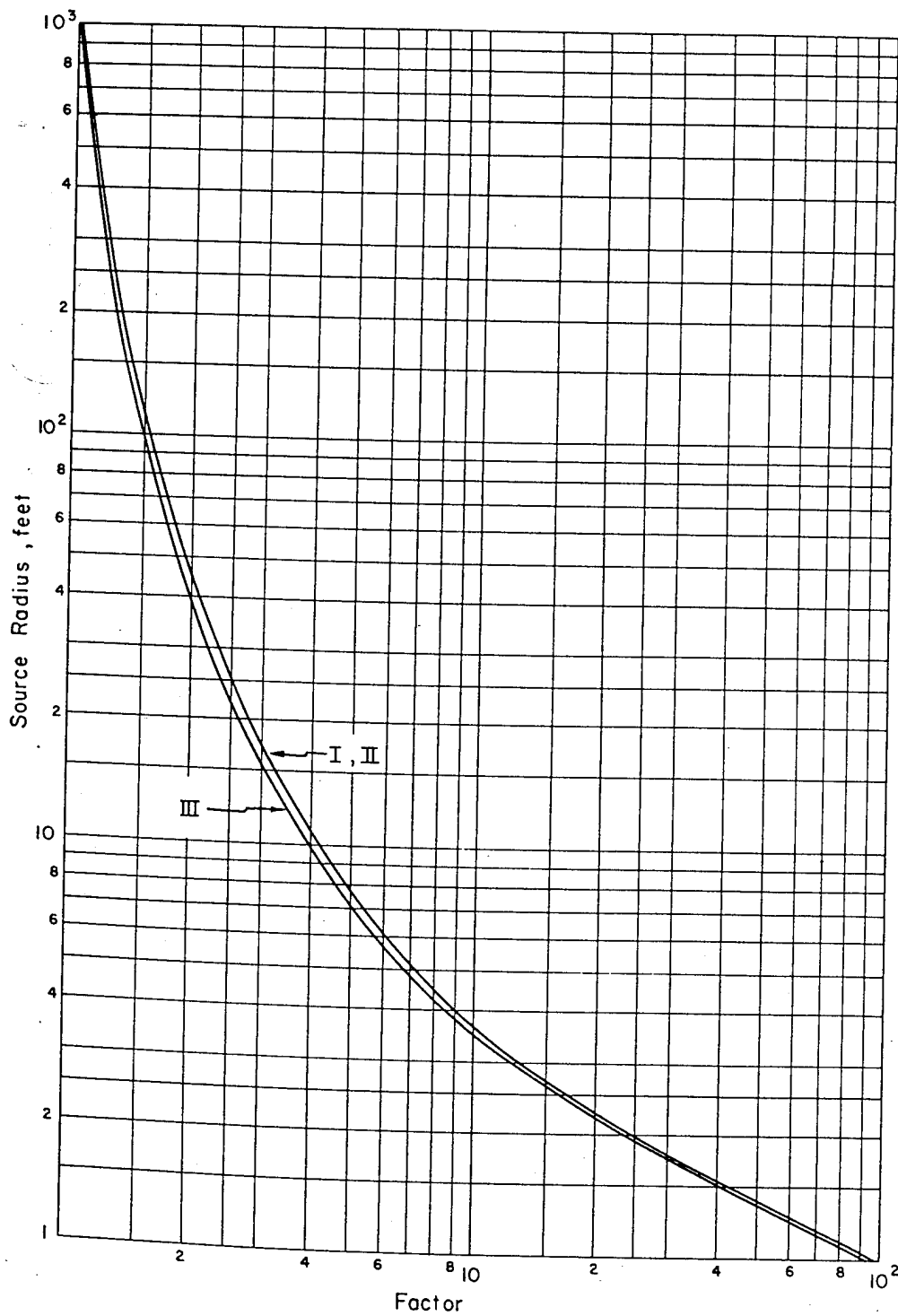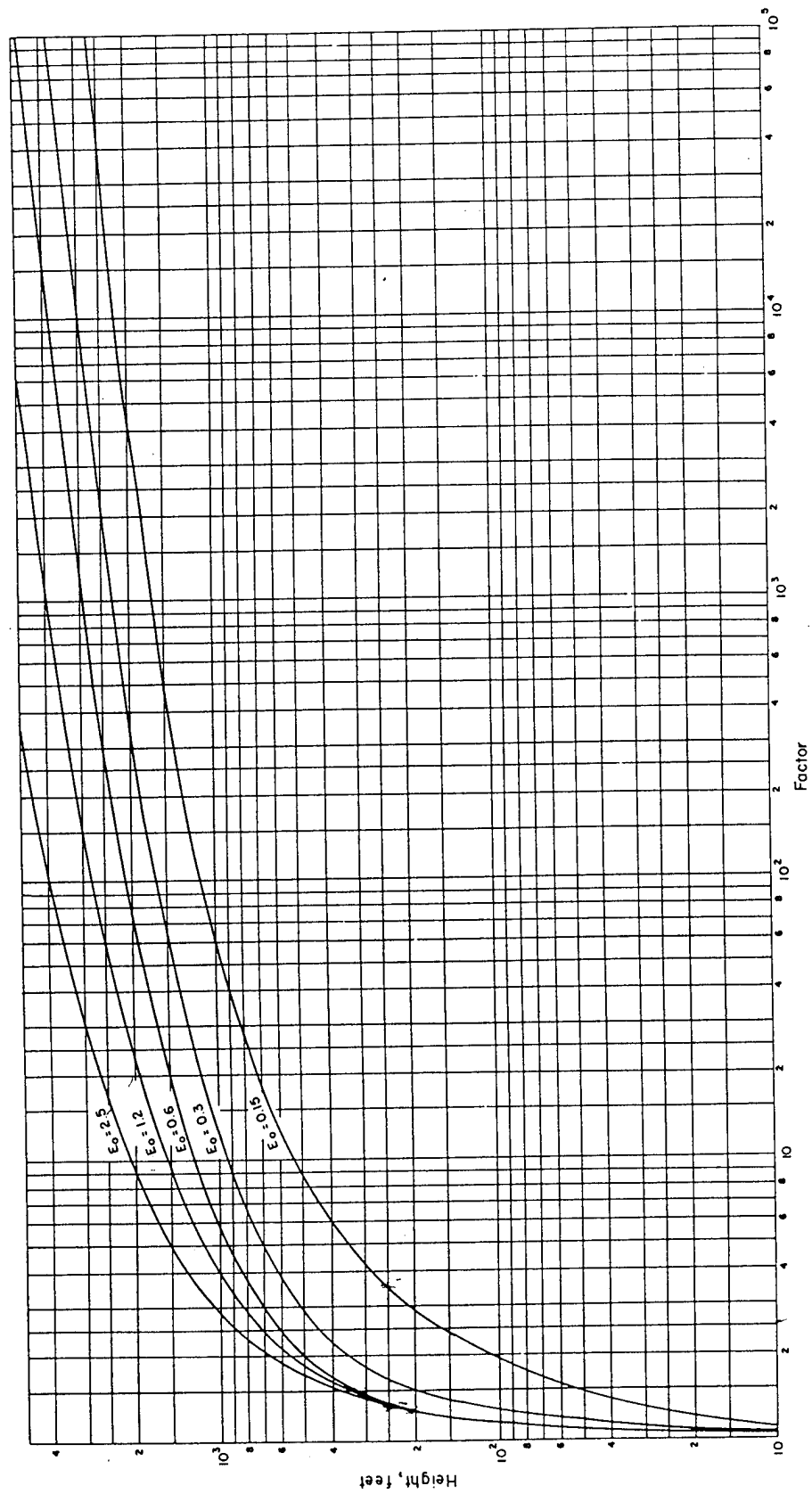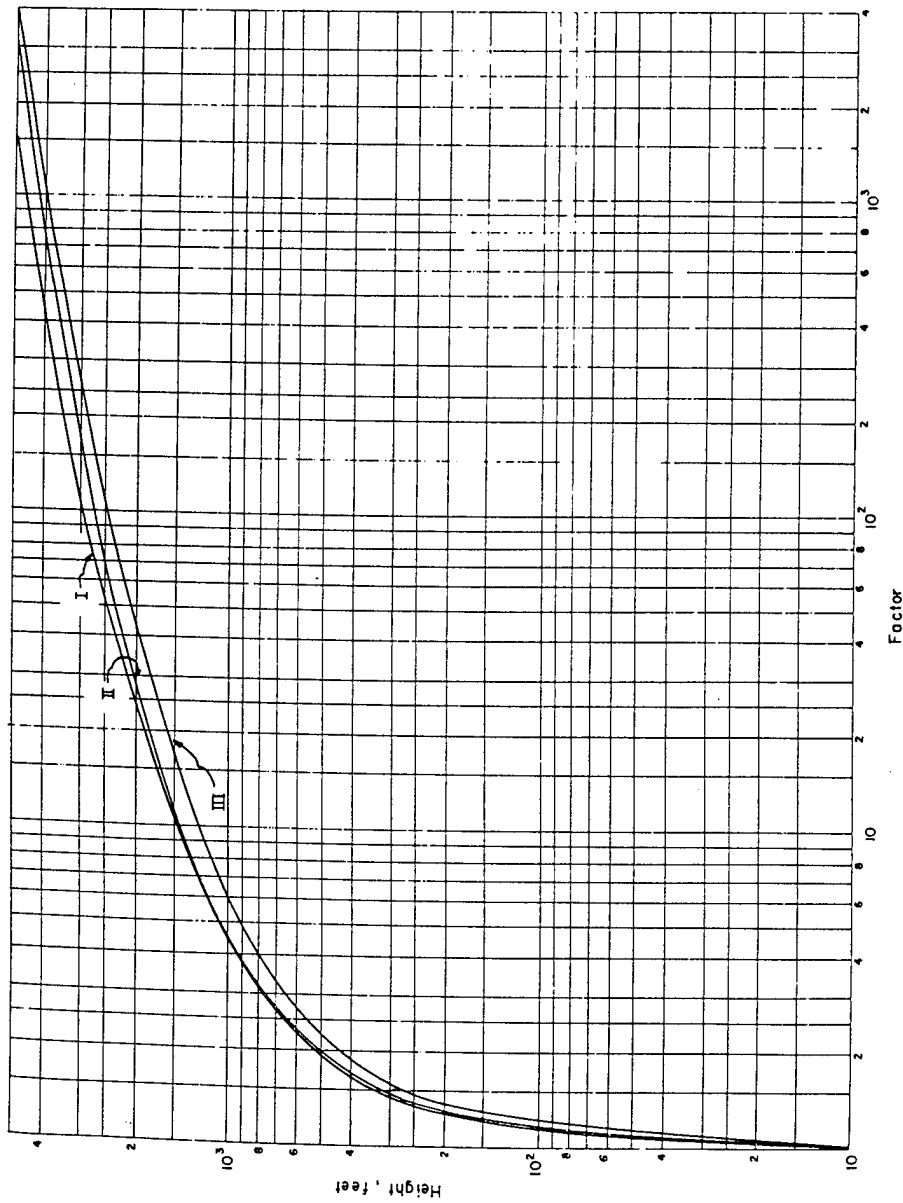The purpose of this report is to provide a calculational background for the gamma-attenuation problem. The calculations represent approximate solutions to certain idealized problems which may or may not apply to practical field conditions. For example, the distribution of radioactive material on land may appear somewhat as a plane distribution, but it is probably modified by irregularities in the surface and leaching into the soil. Only accurate experimental measurements can establish the importance of such effects and, hence, introduce modifications to the calculations.

The numerical calculations have been performed with a desk calculator and were appropriately simplified. The gross division of the energy spectrum could easily be refined by the use of more-elaborate computational equipment. The use of cubic equations to approximate the buildup curves could also be eliminated by the use of high-speed computers. However, in view of the lack of sensitivity of the results to the energy spectrum and the uncertainty in the correlation to practical situations, the curves presented in this report are probably sufficiently accurate.

# REFERENCES

1. Gates, Jr., L.D., and Eisenhauer, C.; Spectral Distribution of Gamma Rays in Air; AFSWP Report No. 502A, January 1954; UNCLASSIFIED.

2. Borg, D.C., and Eisenhauer, C.; Spectrum and Attenuation of Initial Gamma Radiation from Nuclear Weapons; AFSWP Report No. 502B, January 1955; SECRET-RESTRICTED DATA.

# DISTRIBUTION

*Military Distribution Categories 5-40 and 5-70*

ARMY ACTIVITIES

1    Asst. Dep. Chief of Staff for Military Operations, D/A, Washington 25, D.C. ATTN: Asst. Executive (R&SW)
2    Chief of Research and Development, D/A, Washington 25, D.C. ATTN: Special Weapons and Air Defense Division
3    Chief of Ordnance, D/A, Washington 25, D.C. ATTN: ORDTX-AR
4- 6    Chief Signal Officer, D/A, P&O Division, Washington 25, D.C. ATTN: SIGOP
7    The Surgeon General, D/A, Washington 25, D.C. ATTN: Chief, R&D Division
8- 9    Chief Chemical Officer, D/A, Washington 25, D.C.
10    The Quartermaster General, D/A, Washington 25, D.C. ATTN: Research and Development Div.
11- 15    Chief of Engineers, D/A, Washington 25, D.C. ATTN: ENGNB
16    Chief of Transportation, Military Planning and Intelligence Div., Washington 25, D.C.
17- 19    Commanding General, Continental Army Command, Ft. Monroe, Va.
20    President, Board #1, Headquarters, Continental Army Command, Ft. Sill, Okla.
21    President, Board #2, Headquarters, Continental Army Command, Ft. Knox, Ky.
22    President, Board #3, Headquarters, Continental Army Command, Ft. Benning, Ga.
23    President, Board #4, Headquarters, Continental Army Command, Ft. Bliss, Tex.
24    Commanding General, First Army, Governor's Island, New York 4, N.Y.
25    Commanding General, Second Army, Ft. George G. Meade, Md.
26    Commanding General, Third Army, Ft. McPherson, Ga. ATTN: ACofS, G-3
27    Commanding General, Fourth Army, Ft. Sam Houston, Tex. ATTN: G-3 Section
28    Commanding General, Fifth Army, 1660 E. Hyde Park Blvd., Chicago 15, Ill.
29    Commanding General, Sixth Army, Presidio of San Francisco, Calif. ATTN: AMGCT-4
30    Commanding General, U.S. Army Caribbean, Ft. Amador, C.Z. ATTN: Cml. Off.
31    Commanding General, USARFANT & MDPR, Ft. Brooke, Puerto Rico
32    Commanding General, Southern European Task Force, APO 168, New York, N.Y. ATTN: ACofS, G-3
33- 34    Commander-in-Chief, Far East Command, APO 500, San Francisco, Calif. ATTN: ACofS, J-3
35    Commanding General, U.S. Army Forces Far East (Main), APO 343, San Francisco, Calif. ATTN: ACofS, G-3
36    Commanding General, U.S. Army Alaska, APO 942, Seattle, Wash.
37- 38    Commanding General, U.S. Army Europe, APO 403, New York, N.Y. ATTN: OPOT Div., Combat Dev. Br.
39- 40    Commanding General, U.S. Army Pacific, APO 958, San Francisco, Calif. ATTN: Cml. Off.
41- 42    Commandant, Command and General Staff College, Ft. Leavenworth, Kan. ATTN: ALLLS(AS)
43    Commandant, Army War College, Carlisle Barracks, Pa. ATTN: Library
44    Commandant, The Artillery and Guided Missile School, Ft. Sill, Okla.
45    Secretary, The Antiaircraft Artillery and Guided Missile School, Ft. Bliss, Texas. ATTN: Maj. George D. Breitegan, Dept. of Tactics and Combined Arms
46    Commanding General, Army Medical Service School, Brooke Army Medical Center, Ft. Sam Houston, Tex.

47    Director, Special Weapons Development Office, Headquarters, CONARC, Ft. Bliss, Tex. ATTN: Capt. T. E. Skinner
48    Commandant, Walter Reed Army Institute of Research, Walter Reed Army Medical Center, Washington 25, D.C.
49    Superintendent, U.S. Military Academy, West Point, N.Y. ATTN: Prof. of Ordnance
50    Commandant, Chemical Corps School, Chemical Corps Training Command, Ft. McClellan, Ala.
51- 52    Commanding General, Research and Engineering Command, Army Chemical Center, Md. ATTN: Deputy for RW and Non-Toxic Material
53    Commanding General, Aberdeen Proving Grounds, Md. (inner envelope) ATTN: RD Control Officer (for Director, Ballistics Research Laboratory)
54- 56    Commanding General, The Engineer Center, Ft. Belvoir, Va. ATTN: Asst. Commandant, Engineer School
57    Commanding Officer, Engineer Research and Development Laboratory, Ft. Belvoir, Va. ATTN: Chief, Technical Intelligence Branch
58    Commanding Officer, Picatinny Arsenal, Dover, N.J. ATTN: ORDBB-TK
59    Commanding Officer, Frankford Arsenal, Philadelphia 37, Pa. ATTN: Col. Tewes Kundel
60    Commanding Officer, Army Medical Research Laboratory, Ft. Knox, Ky.
61- 62    Commanding Officer, Chemical Corps Chemical and Radiological Laboratory, Army Chemical Center, Md. ATTN: Tech. Library
63    Commanding Officer, Transportation R&D Station, Ft. Eustis, Va.
64    Commandant, The Transportation School, Ft. Eustis, Va. ATTN: Security and Information Officer
65    Director, Technical Documents Center, Evans Signal Laboratory, Belmar, N.J.
66    Director, Waterways Experiment Station, PO Box 631, Vicksburg, Miss. ATTN: Library
67    Director, Operations Research Office, Johns Hopkins University, 7100 Connecticut Ave., Chevy Chase, Md. Washington 15, D.C.
68- 69    Commanding General, Quartermaster Research and Development, Command, Quartermaster Research and Development Center, Natick, Mass. ATTN: CBR Liaison Officer
70    Commandant, The Army Aviation School, Ft. Rucker, Ala.
71    President, Board #6, CONARC, Ft. Rucker, Ala.
72- 78    Technical Information Service Extension, Oak Ridge, Tenn.


NAVY ACTIVITIES

79- 80    Chief of Naval Operations, D/N, Washington 25, D.C. ATTN: OP-36
81    Chief of Naval Operations, D/N, Washington 25, D.C. ATTN: OP-03EG
82    Director of Naval Intelligence, D/N, Washington 25, D.C. ATTN: OP-922V
83    Chief, Bureau of Medicine and Surgery, D/N, Washington 25, D.C. ATTN: Special Weapons Defense Div.
84    Chief, Bureau of Ordnance, D/N, Washington 25, D.C.
85    Chief of Naval Personnel, D/N, Washington 25, D.C.
86- 87    Chief, Bureau of Ships, D/N, Washington 25, D.C. ATTN: Code 348
88    Chief, Bureau of Yards and Docks, D/N, Washington 25, D.C. ATTN: D-440
89    Chief, Bureau of Supplies and Accounts, D/N, Washington 25, D.C.
90- 91    Chief, Bureau of Aeronautics, D/N, Washington 25, D.C.
92    Chief of Naval Research, Department of the Navy Washington 25, D.C. ATTN: Code 811

93 Commander-in-Chief, U.S. Pacific Fleet, Fleet Post Office, San Francisco, Calif.
94 Commander-in-Chief, U.S. Atlantic Fleet, U.S. Naval Base, Norfolk 11, Va.
95-98 Commandant, U.S. Marine Corps, Washington 25, D.C. ATTN: Code AO3H
99 President, U.S. Naval War College, Newport, R.I.
100 Superintendent, U.S. Naval Postgraduate School, Monterey, Calif.
101 Commanding Officer, U.S. Naval Schools Command, U.S. Naval Station, Treasure Island, San Francisco, Calif.
102 Commanding Officer, U.S. Fleet Training Center, Naval Base, Norfolk 11, Va. ATTN: Special Weapons School
103 Commanding Officer, U.S. Fleet Training Center, Naval Station, San Diego 36, Calif. ATTN: (SPWP School)
104 Commanding Officer, Air Development Squadron 5, VX-5, U.S. Naval Air Station, Moffett Field, Calif.
105 Commanding Officer, U.S. Naval Damage Control Training Center, Naval Base, Philadelphia 12, Pa. ATTN: ABC Defense Course
106 Commanding Officer, U.S. Naval Unit, Chemical Corps School, Army Chemical Training Center, Ft. McClellan, Ala.
107 Commander, U.S. Naval Ordnance Laboratory, Silver Spring 19, Md. ATTN: EH
108 Commander, U.S. Naval Ordnance Laboratory, Silver Spring 19, Md. ATTN: R
109 Commander, U.S. Naval Ordnance Test Station, Inyokern, China Lake, Calif.
110 Officer-in-Charge, U.S. Naval Civil Engineering Res. and Evaluation Lab., U.S. Naval Construction Battalion Center, Port Hueneme, Calif. ATTN: Code 753
111 Commanding Officer, U.S. Naval Medical Research Inst., National Naval Medical Center, Bethesda 14, Md.
112 Director, U.S. Naval Research Laboratory, Washington 25, D.C. ATTN: Mrs. Katherine H. Cass
113 Director, The Material Laboratory, New York Naval Shipyard, Brooklyn, N. Y.
114 Commanding Officer and Director, U.S. Navy Electronics Laboratory, San Diego 52, Calif.
115-118 Commanding Officer, U.S. Naval Radiological Defense Laboratory, San Francisco 24, Calif. ATTN: Technical Information Division
119 Commanding Officer and Director, David W. Taylor Model Basin, Washington 7, D.C. ATTN: Library
120 Commander, U.S. Naval Air Development Center, Johnsville, Pa.
121 Commanding Officer, Clothing Supply Office, Code 1D-0, 3rd Avenue and 29th St., Brooklyn, N.Y.
122 Commandant, U.S. Coast Guard, 1300 E. St. N.W., Washington 25, D.C. ATTN: Capt. J. R. Stewart
123-129 Technical Information Service Extension, Oak Ridge, Tenn. (Surplus)

AIR FORCE ACTIVITIES

130 Asst. for Atomic Energy, Headquarters, USAF, Washington 25, D.C. ATTN: DCS/O
131 Director of Operations, Headquarters, USAF, Washington 25, D.C. ATTN: Operations Analysis
132 Director of Plans, Headquarters, USAF, Washington 25, D.C. ATTN: War Plans Div.
133 Director of Research and Development, Headquarters, USAF, Washington 25, D.C. ATTN: Combat Components Div.
134-135 Director of Intelligence, Headquarters, USAF, Washington 25, D.C. ATTN: AFOIN-IB2
136 The Surgeon General, Headquarters, USAF, Washington 25, D.C. ATTN: Bio. Def. Br., Pre. Med. Div.
137 Deputy Chief of Staff, Intelligence, Headquarters, U.S. Air Forces Europe, APO 633, New York, N.Y. ATTN: Directorate of Air Targets
138 Commander, 497th Reconnaissance Technical Squadron (Augmented), APO 633, New York, N.Y.
139 Commander, Far East Air Forces, APO 925, San Francisco, Calif.
140 Commander-in-Chief, Strategic Air Command, Offutt Air Force Base, Omaha, Nebraska. ATTN: Special Weapons Branch, Inspector Div., Inspector General
141 Commander, Tactical Air Command, Langley AFB, Va. ATTN: Documents Security Branch
142 Commander, Air Defense Command, Ent AFB, Colo.
143-144 Research Directorate, Hdqs. Air Force Special Weapons Center, Kirtland Air Force Base, New Mexico. ATTN: Blast Effects Research

145 Assistant Chief of Staff, Installations, Headquarters, USAF, Washington 25, D.C. ATTN: AFCIE-E
146 Commander, Air Research and Development Command, PO Box 1395, Baltimore, Md. ATTN: RDDN
147 Commander, Air Proving Ground Command, Eglin AFB, Fla. ATTN: Adj./Tech. Report Branch
148-149 Director, Air University Library, Maxwell AFB, Ala.
150-157 Commander, Flying Training Air Force, Waco, Tex. ATTN: Director of Observer Training
158 Commander, Crew Training Air Force, Randolph Field, Tex. ATTN: 2GTS, DCS/O
159-160 Commandant, Air Force School of Aviation Medicine, Randolph AFB, Tex.
161-163 Commander, Wright Air Development Center, Wright-Patterson AFB, Dayton, O. ATTN: WCOSI
164-165 Commander, Air Force Cambridge Research Center, LG Hanscom Field, Bedford, Mass. ATTN: CRQST-2
166-168 Commander, Air Force Special Weapons Center, Kirtland AFB, N. Mex. ATTN: Library
169-170 Commander, Lowry AFB, Denver, Colo. ATTN: Department of Armament Training
171 Commander, 1009th Special Weapons Squadron, Headquarters, USAF, Washington 25, D.C.
172-173 The RAND Corporation, 1700 Main Street, Santa Monica, Calif. ATTN: Nuclear Energy Division
174 Commander, Second Air Force, Barksdale AFB, Louisiana. ATTN: Operations Analysis Office
175 Commander, Eighth Air Force, Westover AFB, Mass. ATTN: Operations Analysis Office
176 Commander, Fifteenth Air Force, March AFB, Calif. ATTN: Operations Analysis Office
177 Commander, Western Development Div. (ARDC), PO Box 262, Inglewood, Calif. ATTN: WDSIT, Mr. R. G. Weitz
178-184 Technical Information Service Extension, Oak Ridge, Tenn. (Surplus)

OTHER DEPARTMENT OF DEFENSE ACTIVITIES

185 Asst. Secretary of Defense, Research and Development, D/D, Washington 25, D.C. ATTN: Tech. Library
186 U.S. Documents Officer, Office of the U.S. National Military Representative, SHAPE, APO 55, New York, N.Y.
187 Director, Weapons Systems Evaluation Group, OSD, Rm 2E1006, Pentagon, Washington 25, D.C.
188 Commandant, Armed Forces Staff College, Norfolk 11, Va. ATTN: Secretary
189-194 Commanding General, Field Command, Armed Forces Special Weapons Project, PO Box 5100, Albuquerque, N. Mex.
195-196 Commanding General, Field Command, Armed Forces, Special Weapons Project, PO Box 5100, Albuquerque, N. Mex. ATTN: Technical Training Group
197-201 Chief, Armed Forces Special Weapons Project, Washington 25, D.C. ATTN: Documents Library Branch
202-208 Technical Information Service Extension, Oak Ridge, Tenn. (Surplus)

ATOMIC ENERGY COMMISSION ACTIVITIES

209-211 U.S. Atomic Energy Commission, Classified Technical Library, 1901 Constitution Ave., Washington 25, D.C. ATTN: Mrs. J. M. O'Leary (For DMA)
212-213 Los Alamos Scientific Laboratory, Report Library, PO Box 1663, Los Alamos, N. Mex. ATTN: Helen Redman
214-218 Sandia Corporation, Classified Document Division, Sandia Base, Albuquerque, N. Mex. ATTN: Martin Lucero
219-221 University of California Radiation Laboratory, PO Box 808, Livermore, Calif. ATTN: Margaret Edlund
222 Weapon Data Section, Technical Information Service Extension, Oak Ridge, Tenn.
223-264 Technical Information Service Extension, Oak Ridge, Tenn. (Surplus)

ADDITIONAL DISTRIBUTION

265 Commander, 1352 Motion Picture Squadron, Lookout Mountain Laboratory, 8935 Wonderland Ave., Los Angeles 46, Calif.

38